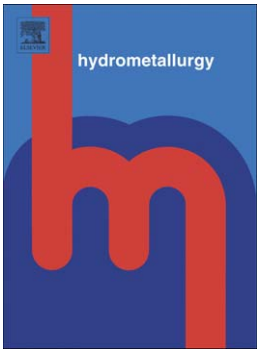

Specific iron oxidation and cell growth rates of bacteria in batch culture

R.M. Candy, K.R. Blight, D.E. Ralph

PII: S0304-386X(09)00082-6
DOI: doi: 10.1016/j.hydromet.2009.04.013
Reference: HYDROM 2993

To appear in: *Hydrometallurgy*

Received date: 5 February 2009
Revised date: 9 April 2009
Accepted date: 14 April 2009

Please cite this article as: Candy, R.M., Blight, K.R., Ralph, D.E., Specific iron oxidation and cell growth rates of bacteria in batch culture, *Hydrometallurgy* (2009), doi: 10.1016/j.hydromet.2009.04.013

Specific iron oxidation and cell growth rates of bacteria in batch culture

R.M. Candy, K.R. Blight and D.E. Ralph*

AJ Parker CRC for Integrated Hydrometallurgical Solutions, School of Chemical and Mathematical Sciences, Murdoch University, South Street, Murdoch, 6150, Western Australia.

*Corresponding author. D.Ralph@murdoch.edu.au

ABSTRACT

The increase in cell number during a batch culture cycle of iron oxidizing bacteria was measured by an optical probe that operated on the principle of light scattering by cells within the optical path. These data together with the redox potential measured in the growth media allowed the parameters of culture activity, specific substrate oxidation and cell replication rates to be determined throughout the cycle. The technique was used to examine the effect of increased ionic strength by addition of sodium sulfate to minimal iron media. Both the presence of excess sulfate and the potential of the iron couple at the time of inoculation were shown to affect the first half of the batch culture cycle where the potential of the iron couple was less than 0.65 V. Addition of sulfate above the minimal media values did not produce any adverse effects on cell activity when the potential of the iron couple was greater than 0.65 V. The complexation or inhibition of the iron-centred components of the electron transport chain is proposed to explain the observed specific substrate oxidation rates. The yield of cells produced from a given amount of substrate was not significantly affected by sulfate addition. Rates of substrate utilisation and yield were directly compared to values obtained by other workers.

Keywords: Iron oxidising bacteria; Specific growth rates; Specific substrate utilisation rates; Bio-oxidation; Ionic strength:

1. Introduction

Batch culture offers a simple and convenient method to study the growth of acidophilic iron oxidising bacteria. These cells are important in bio-hydrometallurgical processes for the recovery of metals from sulfidic minerals. Our group has been focussed on the impact of process water quality on the growth and activity of these cells. To facilitate this study, optical methods were developed to continuously monitor cell numbers throughout a batch

culture cycle. Knowledge of the cell population in conjunction with measurements of the redox potential of the Fe^{3+}/Fe^{2+} couple in the medium can be used to derive kinetic data.

Solutions of high concentration and therefore ionic strength (*I*) are usually favoured for hydrometallurgical processes as less process solution and bulk handling are required to recover a given mass of product. However, this is not necessarily the case for bio-hydrometallurgical processes. It is clear that increasing *I* either by increasing substrate concentration or by addition of background electrolyte ions makes a significant difference to the growth of lithotrophic bacteria (Blight and Ralph, 2004; Sundkvist et al., 2007) and must be considered when predicting the activity of cells. Ionic strength is not considered in the Monod model or its various derivations (Ojumu et al., 2006; Nemati et al., 1998). The effects of changing Fe^{2+} and Fe^{3+} concentrations have been modelled in terms of substrate and product inhibition (Jones and Kelly, 1983) but descriptions of the effect of background electrolytes such as sodium sulfate are limited (Shiers et al., 2005; Blight and Ralph, 2004).

The motivation for developing an optical method stems from the difficulty in measuring lithotrophic bacterial cell numbers by conventional methods. The amount of cell mass produced from oxidation of Fe^{2+} is low compared to the mass yield for heterotrophic cells and so gravimetric methods cannot be readily applied. Cell counts are tedious and subject to significant uncertainty, whilst methods that quantify a cell component such as total protein or ATP are available but not readily automated. Light occlusion and scattering by bacterial cells has been used for quantitative analysis of cell populations (Robrish et al., 1971; Trotman, 1978). The technique was applied in this study to continuously monitor cell numbers. These data were then used to determine the specific rates of substrate oxidation and cell replication and to observe the effect of *I* on these variables.

The activity of lithotrophic bacteria has been studied using a variety of culture methods, generally with the focus on the specific rate of substrate utilisation as a function of solution

parameters. Predictive models of growth and activity show good agreement in the region where $1 < [Fe^{3+}]/[Fe^{2+}] < 100$ using only $[Fe^{3+}]$, $[Fe^{2+}]$ and pO_2 as input variables (Ojumu et al., 2006). The agreement between quantitative models for rates of substrate utilisation in the region where $[Fe^{3+}]/[Fe^{2+}] < 1$ is less convincing due in part to the difficulties in operating a continuous culture of iron oxidising organisms under that condition. Meruane et al. (2002) used a 'potentiostat' apparatus to show that the specific rate of substrate utilisation increased linearly as the potential of the iron couple ($E_{III/II}$) was reduced below 0.66 V. Their model was based on electrochemical principles using values of $E_{III/II}$ rather than concentration or activity of the Fe^{3+} and Fe^{2+} species as input data (ibid). However, none of the other models reviewed by Ojumu et al. (2006) were structured to include effects of *I* on activity of the Fe^{3+} and Fe^{2+} species.

A barrier to comparing reported rates of specific substrate utilisation arises from the methods used to determine cell numbers or mass. This problem can be solved by gas analyses (Breed et al., 1999; Ojumu et al., 2008) where the amount of carbon fixed into biomass is found from the difference between input and exhaust CO_2 concentrations in the gas stream. Biomass in these studies has the unit 'C-mol' (or mmol-C), which gives the number or mass of cells containing 12.0 g of carbon. Sundkvist et al. (2007) used protein analysis to determine biomass, generating the unit of μg (protein). The optical probe methods used in this study determined biomass as cell numbers per unit volume (N). Equivalence factors of cell carbon mass fraction and cell number per unit mass have been reported (Blight and Ralph, 2008) these allow a comparison of the same organism parameters determined using different methods.

2. Experimental

2.1 Equipment and materials

All chemicals used in this study were analytical grade reagents (AR) unless otherwise stated and all solutions were prepared with distilled water. The chemolithotrophic organisms used in previous studies (Blight and Ralph, 2004; Shiers et al., 2005; Blight and Ralph, 2008 and 2008a) were used as inocula for these experiments. A pH meter (Metrohm model 691) and glass membrane electrode calibrated against pH 1.68 and 3.65 buffers was used to measure pH. Temperature correction was applied in all calibration and measurement procedures. Cell counts were performed using a Hauser hemocytometer with a grid area of 2.5×10^{-3} mm^2 and a volume of 2.5×10^{-10} L. The redox probe was constructed from a 0.5 mm diameter platinum wire and a $Ag/AgCl_{(satd.\ KCl)}$ reference electrode and calibrated following the procedure described earlier (Blight and Ralph, 2004). A standard hydrogen electrode (SHE) was used to monitor the performance of the Ag/AgCl reference electrode which throughout the study gave a consistent E value of 0.203 V against the SHE. The construction and operation of the optical probe has been described elsewhere (Candy, 2008). Data from the probes during batch culturing experiments were recorded at 10 minute intervals as instantaneous values.

2.2 Growth media

Three component solutions were prepared in bulk and used to produce a minimal growth medium as required. Solution A, a sulphuric acid solution was prepared by adding concentrated H_2SO_4 to deionised water until a pH of 1.50 ± 0.05 was obtained. Solution B, a macro-nutrient solution was prepared from the following salts, $(NH_4)_2SO_4$ (5.00 g), K_2HPO_4 (2.50 g), $MgSO_4.7H_2O$ (2.50 g) and $CaCl_2.0.5H_2O$ (0.100 g) dissolved in 1.00 L of deionised water and adjusted to pH 1.50 ± 0.05 with concentrated H_2SO_4. Solution C, a solution of micro-nutrients was prepared from the following salts, $CoSO_4.7H_2O$ (2.49 g), $CuSO_4.7H_2O$ (2.81 g), $MnSO_4.H_2O$ (1.69 g), $(NH_4)_6Mo_7O_{24}.4H_2O$ (1.77 g), $NiSO_4.6H_2O$ (2.62 g) and

$ZnSO_4.7H_2O$ (2.87 g) dissolved in 1.00 L of deionised water and adjusted to pH 1.50 ± 0.05 with concentrated H_2SO_4.

Minimal medium for batch cultures (1.0 L) was prepared by dissolving AR grade $FeSO_4.7H_2O$ (20.00 g) in the sulphuric acid solution A. Macro-nutrient solution B (100 mL) and micro-nutrient solution C (1.00 mL) were added and the solution diluted to 990 mL with sulphuric acid solution A. The required amount of solid anhydrous Na_2SO_4 was added, dissolved, and the pH adjusted with concentrated H_2SO_4 to pH 1.60 ± 0.05 followed by dilution to 1.00 L with sulphuric acid solution A. All media were filtered through 0.45 μm membranes before use.

2.3 Growth experiments

Four media M00, M10, M20 and M40 were prepared with 0, 10, 20 and 40 g L^{-1} sodium sulfate respectively, and were used to maintain separate sequences of 100 mL batch cultures to provide a ready source of inocula. These cultures were inoculated into fresh media every 2 or 3 days and also used to inoculate the 1.0 L or 5.0 L reactors. Both the 5.0 L and 1.0 L reactors were stirred, sparged with air and maintained at 35°C. Cells were harvested from completed 5.0 L batches and re-suspended in solution A. This slurry was used to calibrate the optical probe. The 1.0 L reactor was charged with medium, the probes inserted and the reactor bought to temperature inside a light–proof cover. Cells from the appropriate 100 mL batch were harvested, re-suspended in solution A and added to the reactor when the optical probe response was stable. Each experiment reported has a unique number and a title, e.g. M00-17 refers to experiment number 17 conducted using the standard medium without any added sodium sulfate.

243 Light probe calibration

Bacterial cell numbers were estimated using an optical probe to measure changes in the light intensity transmitted through the solution. The probe was immersed in the reactor fluid and had a red LED light source (λ_{max} 638 nm) in direct alignment with a photo-sensitive detector at a constant path length of 50 mm. The probe was sensitive to reactor temperature, the background colour produced by soluble ferric species, ambient light as well as bacterial cells and precipitated iron solids. Before each experiment the probe was calibrated by growing large numbers of cells in 5 L of the medium of interest, harvesting the cells and re-suspending them in solution A to form a slurry. Aliquots of known volume of the slurry were added to the reactor charged with solution A and the optical probe response recorded. Cell numbers were counted after the addition of each aliquot. The plot of slurry volume and cell numbers (N) against the probe's transducer voltage change (V) was linear for each calibration ($R^2 > 0.994$, Candy, 2008) but differed between experiments with cells grown in the same media and between experiments with cells grown in different media (mean of 8 calibrations in the four media $N/V = 1.58\times10^9$ cell L^{-1} mV^{-1}, $s = 3.8\times10^8$).

Depending on the pH, the oxidation of ferrous ions produced a soluble coloured ferric species with λ_{max} at 308 nm (Basaran and Tuovinen, 1986); but with significant absorbance at 638 nm, it was necessary to apply a correction for this background attenuation. This was achieved for each medium by titrating fresh uninoculated medium with 10% H_2O_2 (30% v/v diluted with solution A) with both the optical and redox probes in place to obtain a plot of the optical probe voltage change against the platinum electrode potential ($E_{III/II}$). The probe's response to the change in colour was hyperbolic with respect to $E_{III/II}$, but was linear with respect to Fe^{3+} concentration and was reduced as the concentration of sodium sulfate

increased. At 40 g L^{-1} sulfate (M40) the optical probe response was insignificant as $E_{III/II}$ increased and was neglected. But in other media, a function linking $E_{III/II}$ and voltage response, was applied (Candy, 2008). A plot of $E_{III/II}$ against the titrant volume yielded values for the constants in equation 1 (table 1) using the procedure reported earlier (Blight and Ralph, 2004).

2.5 Integrating batch culture data

Throughout this analysis the activities of the Fe^{2+} and Fe^{3+} species are referred to as II and III while their derivatives with respect to time are dII/dt and dII/dt respectively. Values for the rates of dII/dt and dN/dt as well as the specific rates (dII/dt)/N and (dN/dt)/N were derived from the Fe^{2+} substrate and cell concentration data (II and N respectively). The $E_{III/II}$ *vs.* time data collected from the platinum electrode was integrated by triangulation to yield dE/dt. Using the constants in Table 1 and equations 1, 2 and 3, the values for II and dII/dt were determined from $E_{III/II}$ (May et al., 1997).

$$II = \frac{\Sigma}{1+\exp(\ )} \qquad 1.$$

$$\frac{dII}{dE} = \frac{\frac{\Sigma F}{RT}\exp(\ )}{(1+\exp(\ ))^2} \qquad 2.$$

$$\frac{dII}{dt} = \frac{dE}{dt}\frac{dII}{dE} \qquad 3.$$

- where Σ is the total iron concentration and assumed to be constant, II is $[Fe^{2+}]$, and exp( ) = $e^{(F(E-E°)/RT)}$ - where E the measured potential of the platinum electrode ($E_{III/II}$) and $E°$ the standard reduction potential of the iron couple in the medium (Table 1) and T was 308.15 K.

Background correction was applied to the raw optical probe data before conversion into units of (N) cells L^{-1}. The data set N *vs.* time was integrated by triangulation to yield dN/dt and (dN/dt)/N.

3. Results

3.1 Batch cultures in M00 medium

Growth in media with no added sodium sulfate proceeded rapidly resulting in decreased substrate concentration with a corresponding increase in cell numbers (Fig.1). No appreciable 'lag phase' was observed, although the period required to complete batch culture cycles varied by up to 10 hours. This variation is due to the difference in inocula cell numbers and initial $E_{III/II}$ values of the media. The concentration of cells at t = 0 varied from 2.6×10^8 cells L^{-1} (M00-20) to 30×10^8 cells L^{-1} (M00-24) and $E_{III/II}$ at inoculation varied over the range of 0.56 - 0.59 V (Table 2).

Table 2 gives the inoculum size, initial $E_{III/II}$ values for each experiment and time required to utilise half the available substrate. Faster substrate utilisation occurred if the number of cells in the inoculum was increased (*cf.* M00-24 and M00-26, M00-17 and M00-22). However, lower initial $E_{III/II}$ values led to lower utilisation rates, even if the number of cells in each inoculum was similar (*cf.* M00-23 and M00-26).

3.2 Specific substrate utilisation rate in M00 media

The specific substrate utilisation rates {(dII/dt)/N} derived for the above six experiments (Table 2) are shown in Figs. 2 and 3 as a function of substrate concentration (II) and $E_{III/II}$ value. The Monod relationship linking (dII/dt)/N and II can be used with reasonable success to describe (dII/dt)/N as a function of substrate concentration in the latter stages of the batch culture cycle. However, it can be seen from Fig. 2 that the experimental data departs from the Monod model in initial stage of the batch cycle. In every experiment the initial values of dII/dt and dN/dt were relatively high. This effect, seen in Figs 2 and 3, is possibly an artefact of the inoculum transfer as the cells are removed from an environment where the III/II ratio is high ($E_{III/II}$ = 0.80 V) to a medium where that ratio is much smaller ($E_{III/II}$ = 0.55 V). It is expected that Fe^{3+} will desorb and Fe^{2+} adsorb onto the cell surface resulting in artificially elevated dII/dt values. However, the effect was observed even if the inoculum size was reduced by a factor of *ca*. 6 (*cf*. M00-20 and M00-24). It is likely that the initial behaviour of (dII/dt)/N after inoculation was dependent on the value of $E_{III/II}$ at the time of inoculation.

The area under the curve is a measure of the total charge passed by the III/II couple through the cell membrane and in the initial stage of the batch culture, this varies significantly with the inoculation value of $E_{III/II}$. It can be seen from Fig.3 that the high initial rates of (dII/dt)/N fall rapidly when the initial $E_{III/II}$ value is low (M00-17, M00-20 and M00-23); and fall slowly when the initial $E_{III/II}$ value is higher (M00-22, M00-24 and M00-26). However, by the time the substrate concentration had fallen by half ($E_{III/II}$ = 0.65 V) the patterns of (dII/dt)/N vs. II (or $E_{III/II}$) were identical.

The effect of the initial $E_{III//II}$ value appears almost counter-intuitive because inoculation at lower values of $E_{III/II}$ result in lower values of (dII/dt)/N; i.e. a larger potential difference from which the cell can extract energy, gives rise to a lower flux of charge through the cell membrane. Furthermore, as the $E_{III/II}$ rises after inoculation the values for (dII/dt)/N remain lower than those exhibited by cells introduced at the higher $E_{III/II}$.

Literature values for (dII/dt)/N were collated and converted to units that allow a direct comparison with data from these experiments (Table 3). Where the authors have quoted a range for (dII/dt)/N, intermediate values were used. It can be seen that the agreement between different methods is reasonable.

3.3 Cell doubling rate constant in M00 media

The effect of $E_{III//II}$ on the cell doubling rate constant {(dN/dt)/N} is shown in Fig. 4. Inoculation at lower $E_{III/II}$ values also results in lower values of (dN/dt)/N for the initial stages of the batch cycle. However, by $E_{III/II}$ = 0.65 V the specific rates of cell production in all cultures were similar. Towards the end of the batch cycle, when $E_{III/II}$ > 0.80 V and the substrate is near exhaustion, a solid Fe(III) phase begins to form resulting in higher apparent values of (dN/dt)/N.

3.4 Yield values in M00 media

The data from the experiments using M00 media were interpreted following the Pirt model (equation 4) by plotting (dII/dt)/(dN/dt) against N/(dN/dt) (Fig. 5).

$$1/Y_{obs} = m/\mu + Y_{max} \qquad 4.$$

The specific growth rate term μ (h^{-1}) used by Pirt (1975) corresponds directly to the term (dN/dt)/N (h^{-1}) used in this study. The value derived here for Y_{max} has dimensions of mol $cell^{-1}$ and the maintenance energy (*m*) units of mol $cell^{-1}$ h^{-1} rather than a mass of biomass or a number of mole of carbon. The conversion factors are given in Table 3.

The value for Y_{max} derived from the Pirt equation for cells in M00 media (Fig. 5) was 1.7×10^{12} cell.mol^{-1} corresponding to 4.7 mg.cells g^{-1} iron, 2.0×10^{-4} C-mol g^{-1} or 1.1×10^{-2} C-mol mol^{-1}. The *m* value derived was 4×10^{-14} mol.cell^{-1} h^{-1}. The fit of these data to the Pirt model ($R^2 = 0.65$) can only be achieved by not considering any data points where N/(dN/dt) > 30 ($\mu = 0.03$ h^{-1}). It is concluded that the Pirt model is of questionable value for the thermodynamic analysis.

Blight and Ralph (2008) proposed that Y_{max} varies throughout a batch culture cycle as the $E_{III/II}$ value changes. Figs 6 and 7 present the instantaneous values of the observed yield {Y_{obs}, (dN/dt)/(–dII/dt)} as a function of II and $E_{III/II}$ respectively. The theoretical maximum thermodynamic yield (Y_{max}) is plotted on the secondary axis in same units but with a different scale. The trend of Y_{obs} was to decrease over the batch cycle as the value of $E_{III/II}$ increased. In the final stages of each batch cycle Y_{obs} rapidly increased due to formation of Fe(III) oxide solids. Disregarding data from the initial stages and final stages of the cycle, reveals a pattern where Y_{obs} is approximately constant at 1.1×10^{12} cells mol^{-1} (0.18 g mol^{-1}, 0.0073 C-mol mol^{-1}, and 3.1 mg g^{-1}) when $0.57 < E_{III/II} < 0.67$ and declines as $E_{III/II}$ increases beyond 0.67 V parallelling the predicted decline in Y_{max}.

Neither the Pirt model (1975) nor the model proposed by Blight and Ralph (2008) provide an adequate explanation of the observed data. The value of the Y_{obs}/Y_{max} ratio in Fig. 7 at $E_{III/II} = 0.67$ V indicates a thermodynamic growth efficiency of *ca.* 20% which is maintained through the latter stages of the batch cycle. Efficiency is lower in the early stages of the cycle when $E_{III/II} < 0.67$ V.

3.5 Effect of sodium sulfate in the medium

Iron oxidation proceeded in the presence of sodium sulphate and only a short 'lag' phase was evident in M10 medium; extending to 24 hours in M20 and *ca.* 100 hours in M40 media respectively. The addition of sulfate resulted in the initial value of $E_{III/II}$ decreasing as the concentration increased (Table 1). This is an artefact of the relative affinity of SO_4^{2-} for Fe^{3+}. It was possible to inoculate M10, M20 and M40 media at decreasing $E_{III/II}$ values; the resultant patterns of cells numbers and substrate usage are shown in Fig. 8. It can be seen that regardless of the inoculum size, as the initial value $E_{III/II}$ decreased the effect of extra sulfate was to produce longer lag phase periods.

A number of replicate experiments were carried out at each sodium sulfate loading in which the number of cells in the inoculum and initial $E_{III/II}$ values were varied. As shown in Fig. 9 the 'lag phase' at a sodium sulfate concentration of 10 g L^{-1} (M10) was reduced when the initial $E_{III/II}$ value was high (0.57 V, M10-41) and increased when the $E_{III/II}$ value was lower (0.54 V, M10-39 and M10-31 respectively). Experiments M10-31 and M10-41 received similar inocula 0.6 and 0.7×10^8 cells L^{-1} with inoculation at 0.54 and 0.57 V respectively, the resultant periods for completion of half the batch culture cycle were 40 and 28 hours respectively.

The specific substrate oxidation rates in M10 medium with 10 g L^{-1} added sodium sulfate provided an interesting comparison to that observed for M00 medium. The initial transitory 'spike' of high (dII/dt)/N values was present in these experiments. It is evident from Fig. 10 that higher initial $E_{III/II}$ values at inoculation lead to higher values of (dII/dt)/N. After inoculation at low $E_{III/II}$, a maximum for (dII/dt)/N at *ca.* 0.68 V was observed. These patterns were repeated in all experiments with added sulfate. Fig. 11 shows the representative experiments from Fig. 8 at each sulfate concentration with progressively lower media $E_{III/II}$ values at inoculation.

Below 0.68 V there is a difference between (dII/dt)/N values for cells in media with and without additional sulfate. The difference only occurs when $E_{III/II}$ < 0.68 V, above this value the specific rate of substrate usage does not appear to be affected by addition of sulfate. In media with excess sodium sulfate, the amount added makes no significant difference to (dII/dt)/N values provided inoculation occurs at similar $E_{III/II}$ values (Fig. 12). The overall pattern of (dII/dt)/N, observed in the presence of extra sulfate, resembles a 'Gaussian' curve with a maximum at ~0.68 V and minima as $|E_{III/II} - 0.68| > 0.1$ V. The data presented in Fig. 12 and that reported by Ojumu et al. (2006) are strikingly similar. From a potential $E_{III/II}$ > 0.68 V ($[Fe^{3+}]/[Fe^{2+}] > 1$) the sigmoid decline in (dII/dt)/N is similar to those data shown by Ojumu et al. (ibid).

4.0 Discussion

4.1 Examination of colligative effects

In seeking a simple explanation for these observations, we considered the colligative effects of ions in solution. The inclusion of sodium sulfate in iron media could affect bacterial activity without crossing the membrane or directly interfering with the external electron transport chain processes. It is expected that increased *I* external to the cell will result in an increased osmotic pressure gradient across the cell membrane, requiring more energy to maintain cytoplasmic homeostasis and leaving less energy available for fixation of CO_2. Changes in Y_{obs} should result.

Data from Millero et al. (2003) indicate that the oxygen solubility may be reduced by *ca.* 20% in M40 compared to M00 media; presumably the salting effect also lowers CO_2 activity. The observed changes could be caused by lowered gas solubility if oxygen or carbon dioxide

were limiting. The salting effect can be examined by calculating the fluxes and concentration gradients of O_2 and CO_2 that are required to maintain the observed level of cell activity. In M00 media, cells in these experiments showed characteristic (dII/dt)/N values of *ca.* 1.0×10^{-13} mol cell^{-1} h^{-1}. Assuming 5% of this total electron flux reduces CO_2 while the remainder reduces O_2, the fluxes are:

(dII/dt)/N = 1.0×10^{-13} mol(II) cell^{-1} h^{-1} = 2.8×10^{-17} mol cell^{-1} s^{-1}

(dO_2/dt)/N = 2.4×10^{-14} mol(O_2) cell^{-1} h^{-1} = 6.6×10^{-18} mol cell^{-1} s^{-1}

(dCO_2/dt)/N = 1.2×10^{-15} mol(CO_2) cell^{-1} h^{-1} = 3.3×10^{-19} mol cell^{-1} s^{-1}

The mass transfer to small solid particles such as iron oxidizing bacteria is well described (Geankoplis, 1983) and can be represented by equation 5.

$$k_L = \frac{2D_{AB}}{D_P} + 0.31N_{Sc}^{-2/3}\left(\frac{\Delta\rho\mu_C g}{\rho_c^2}\right)^{1/3} \qquad .5$$

The second term describes buoyancy due to gravity and the density difference between the bacterium and the surrounding medium; in this case, the term can be neglected because of the small value of $\Delta\rho$. The D_{AB} is the diffusivity of oxygen and carbon dioxide in water (3.25×10^{-9} and 2.4×10^{-9} m^2 s^{-1} respectively, (Lide, 2005)) and D_P is the diameter of the bacterium (D_P = 1.4×10^{-6} m).

$$k_L(O_2) = \frac{2D_{AB}}{D_P} = \frac{2\times3.25\times10^{-9}}{1.4\times10^{-6}} = 4.64\times10^{-3}\ \text{m s}^{-1} \qquad .6$$

$$k_L(CO_2) = \frac{2D_{AB}}{D_P} = \frac{2\times2.4\times10^{-9}}{1.4\times10^{-6}} = 3.43\times10^{-3}\ \text{m s}^{-1} \qquad .7$$

The flux of dissolved gases transported to a bacterium with a surface area of $(4\pi(D_P/2)^2)/3 = 2.05\times10^{-12}$ m^2 are expressed in equations 8 and 9.

J(O_2) = $(6.6\times10^{-18}/2.05\times10^{-12} = 3.2\times10^{-6}$ mol m^{-2} s^{-1} .8

J(CO_2) = $(3.3\times10^{-19}/2.05\times10^{-12} = 1.6\times10^{-7}$ mol m^{-2} s^{-1} .9

Dividing the flux (J) by the mass transfer coefficient (k_L) gives the concentration gradient required to drive oxygen and carbon dioxide flux.

Gradient (O_2) = 3.2×10^{-6} /4.64×10^{-3} = 6.9×10^{-4} mol m^{-3}

Gradient (CO_2) = 1.6×10^{-7} /3.43×10^{-3} = 4.7×10^{-5} mol m^{-3}

The estimated oxygen concentration gradient is 0.3% of the 0.22 mol m^{-3} O_2 saturation concentration and *ca.* 0.5% of the *ca.* 9×10^{-3} mol m^{-3} CO_2 saturation concentration. On this basis we conclude that the salting effect of *I* on gas solubility would impinge on CO_2 uptake before O_2 uptake but is not likely to cause any of the effects observed in these media.

Similarly, it can be calculated that water will be produced inside each cell as a by-product of substrate oxidation at a rate of *ca.* 4.8×10^{-14} mol $cell^{-1}$ h^{-1}. From the molar volume of water (18.8 mL mol^{-1} at 35 °C, (Lide, 2005)) and the interior volume of an 'empty' cell (4×10^{-12} mL $cell^{-1}$), the period required to fill the cell is *ca.* 4.5 hours. Given the relatively short 'filling period' these cells could control their internal water activity by controlling the diffusion rate rather than actively pumping water against the osmotic gradient. Therefore we reasoned neither the salting effect on gas solubility nor osmotic gradients are likely to be rate limiting factors under the conditions of the experiments in this study.

4.2 Complexation effects

The inability to explain the observed patterns of specific substrate utilisation on the basis of colligative properties led us to consider the nature of complexes formed between Fe^{3+} and sulfate ions. Sulfate is known to bind preferentially to Fe^{3+} relative to Fe^{2+}, the effect is to significantly reduce $E_{III/II}$ couple's E° value (Table 1). The external electron transport chain between the Fe(III/II) and O_2/H_2O couples has been intensively studied (Rohwerder et al., 2003; Ingledew and Cobley, 1980; Blake and Shute 1987 and 1994; Brasseur et al., 2004;

Elbehti et al., 1999 and 2000; Malarte et al., 2005) and redox active components have been characterised. These redox mediators appear to have either iron (Castelle et al., 2008) or copper as their redox active centre (Ida et al., 2003; McGinnis et al., 1986; Kyritsis et al., 1995; Giudici-Orticoni et al., 1999). It's reasonable to assume that iron centred mediators are likely to be more affected by sulfate than copper centred mediators as the charge density of the Fe^{3+}-heme structure is expected to be large relative to that of the Cu^{2+}-protein complex. Although sulfate cannot compete with the heme group for outright complexation of iron, it could affect the mediator's efficacy by hindering electron transfer and shifting E° values for the mediator redox couple. Since copper(II/I) sulfate complexes are relatively weak, we suggest that addition of sulfate would not affect either the E° values of mediators with copper redox-active centres or their 'turnover' rates.

Our interpretation of (dII/dt)/N patterns observed in Fig. 12 for M10, M20 and M40 media is that they result from electron transport by components with copper centres while the pattern exhibited in M00 represents the summation of electron transport for copper and iron centred systems. For M10, M20 and M40 media, the values of (dII/dt)/N were all similar and showed the same pattern as $E_{III/II}$ increased (Fig. 12). The 'Gaussian' pattern observed is similar to that expected for a single mediator that rate limits the electron transport chain.

4.2.1 Electron transport by a single redox mediator

If a single mediator (M) with a standard reduction potential of $E_M°$ is external to the cell and limits the rate of electron transport between the iron and oxygen couples, assuming it is under influence of the solution Fe(III/II) couple (Fig. 13), then flux through the mediator should vary as a function of $E_{III/II}$ as shown in Fig. 14.

The rate expressions for electron transfer to and from M are given by equations 10 and 11 respectively. The overall rate of electron transport is limited by the slower of the two reactions.

$rate_1 = k_1\, a_{II}\, a_{Mox}$ .10

$rate_2 = k_2\, a_{Mred}\, a_{Tox}$ .11

Overall rate = minimum ($rate_1$, $rate_2$) .12

- where k_1 and k_2 are the rate constants, a_{II}, a_{Mox}, a_{Mred} and a_{Tox} represent activities of the species involved in each reaction.

Considering the implications of the above rate limiting mechanism in terms of a batch culture cycle, in the initial stages when the Fe(II) concentration is high, the potential of $E_{III/II}$ is less than $E°_M$ consequently M will be reduced. Therefore, the activity of M_{ox} is low and equation 10 limits the overall flux. Toward the end of a batch cycle when $E_{III/II} > E_M°$, M will be predominantly in the oxidised form (M_{ox}), and equation 11 will represent the overall limit of electron flux. The rate of transfer of electrons between iron and oxygen will have the form as shown in Fig. 14, with a maximal rate when $E_{III/II} = E_M°$ and tending to a minimal rate as $|E_{III/II} - E_M°|$ increases. The rate function is not necessarily symmetric around $E_M°$ as the interaction of M_{ox} with Fe(II) may have characteristics different from those between M_{red} and T_{ox}.

4.3 Effect of the initial $E_{III/II}$ value

To our knowledge the sensitivity of (dII/dt)/N to medium $E_{III/II}$ value at inoculation for media with no added sulfate (M00) has not been systematically investigated. The variable pattern in the specific rate of substrate usage when $E_{III/II} < 0.65$ V, stands in contrast to the similarity in observed behaviour when $E_{III/II} > 0.65$ V. We propose that in the potential

region of $E_{III/II}$ < 0.65 V the electron flux is largely carried by iron-centred mediators with $E°_M$ values in the corresponding range. Inoculation of the culture into media with lower $E_{III/II}$ values always results in lower values of (dII/dt)/N relative to the same culture inoculated into media with higher $E_{III/II}$ values. As potential $E_{III/II}$ rises, the mediator 'group' with $E°_M$ ~ 0.68 V, appears to carry the bulk of the electron flux.

5. Conclusions

The period of a batch culture cycle for iron oxidising bacteria is controlled by the medium's $E_{III/II}$ value at the time of inoculation. Inoculation at $E_{III/II}$ = 0.59 V results in a 27-hour cycle, while inoculation of the same medium at 0.56 V results in a 37-hour cycle. Addition of sodium sulfate (40 g L^{-1}) to the medium allows inoculation at lower $E_{III/II}$ values (<0.52 V) and extends the batch cycle period significantly, up to 130 hours. Low specific rates of substrate oxidation were observed when the cells encountered media with low $E_{III/II}$ values and elevated sulfate ion concentration. The inoculation of batch cultures at low potentials result in long lag periods and a low rate of cell reproduction and specific rate of substrate oxidation. Provided that $E_{III/II}$ >0.66 V the presence of excess sodium sulfate (up to 40 g L^{-1}) does not affect the cell activity significantly.

The deleterious effect of sodium sulfate in the region 0.52 < $E_{III/II}$ < 0.66 V is not likely to arise from the increased osmotic gradient associated with increased ionic strength. Neither does it appear to arise from the 'salting' effect that results in lower concentrations of dissolved O_2 and CO_2. Rather, the effect of sulfate on the activity of iron oxidising bacteria appears to be due to its affect on parts of the external electron transport chain operating in the region $E_{III/II}$ < 0.66 V. An elevated concentration of sulfate is deleterious to cells cultured in media with a potential range of $E_{III/II}$ < 0.66 V.; but cell activity in media with a potential

range of $E_{III/II}$ > 0.66 V is not significantly affected. In process operations the impact of extra sulfate arising from oxidation of the reduced sulfur ores will be low provided the operating values of $E_{III/II}$ are held > 0.66 V.

Acknowledgements

The authors wish to thank the AJ Parker CRC for Integrated Hydrometallurgical Solutions for the funding and support provided for Dr. K. Blight and Ms. R. Candy. We also wish to thank our colleagues for many helpful discussions about this subject.

References

Basaran, A.H., Tuovinen, O.H., 1986. An ultraviolet spectrophotometric method for the determination of pyrite and ferrous ion oxidation by *Thiobacillus ferrooxidans*. Applied Microbiology and Biotechnology 24(4), 338-41.

Blake, R.C., Shute, E.A., 1987. Respiratory enzymes of *Thiobacillus ferrooxidans*. J. Biological Chemistry 262(31) 14983-14989.

Blake, R.C., Shute, E.A., 1994. Respiratory enzymes of *Thiobacillus ferrooxidans*. Kinetic Properties of an acid-stable Iron: Rusticyanin oxidoreductase. Biochemistry 33, 9220-9228.

Blight, K.R., Ralph, D.E., 2004. Effect of ionic strength on iron oxidation with batch cultures of chemolithotrophic bacteria. Hydrometallurgy 73, 325-334.

Blight, K.R., Ralph, D.E., 2008. Maximum yield and standard enthalpy of growth of iron oxidizing bacteria. Hydrometallurgy 93, 66 – 71.

Blight, K.R., Ralph, D.E., 2008a. Aluminium Sulphate and Potassium Nitrate Effects on Batch Culture of Iron Oxidising Bacteria. Hydrometallurgy 92, 130-134.

Brasseur, G., Levican, G., Bonnefoy, V., Holmes, D., Jedlicki, E., Lemesle-Meunier, D., 2004. Apparent redundancy of electron transfer pathways via bc1 complexes and terminal oxidases in the extremophilic chemolithoautotrophic *Acidithiobacillus ferrooxidans*. Biochimica et Biophysica Acta, Bioenergetics 1656(2-3), 114-126.

Breed A.W., Dempers C.J., Searby G.E., Gardner M.N., Rawlings D.E., Hansford G.S., 1999. The effect of temperature on the continuous ferrous-iron oxidation kinetics of a predominantly *Leptospirillum ferrooxidans* culture. Biotechnology and Bioengineering 65(1), 44-53.

Candy, RC., 2008. Lithotrophic cultures in minimal iron media. Honours thesis. Murdoch University. Perth, Western Australia.

Castelle, C. Guiral, M. Malarte, G. Ledgham, F. Leroy, G. Brugna, M., Giudici-Orticoni, M-T., 2008. A new iron-oxidizing/O_2-reducing supercomplex spanning both inner and

outer membranes, isolated from the extreme acidophile *Acidithiobacillus ferrooxidans*. Journal of Biological Chemistry 283(38), 25803-25811.

Cox, J.C., Nicholls, D.G., Ingledew, W.J., 1979. Transmembrane electrical potential and trans-membrane pH gradient in the acidophile *Thiobacillus ferrooxidans*. Biochemical Journal 178, 195-200.

Dempers, C.J., Breed, A.W., Hansford, G.S., 2003. The kinetics of ferrous-iron oxidation by *Acidithiobacillus ferrooxidans* and *Leptospirillum ferrooxidans*: effect of cell maintenance. Biochemical Engineering Journal 16(3), 337-346.

Elbehti, A., Nitschke, W., Tron, P., Michel, C., Lemesle-Meunier, D., 1999. Redox components of cytochrome bc-type enzymes in acidophilic prokaryotes.: I. Characterization of the cytochrome bc1-type complex of the acidophilic ferrous ion-oxidizing bacterium *Thiobacillus ferrooxidans*. Journal of Biological Chemistry 274(24), 16760-16765.

Elbehti, A., Brassuer, G., Lemesle-Meunier, D., 2000. First evidence for existence of an uphill electron transfer through bc_1 NADH-Q oxidoreductase complexes of the acidophilic obligate chemolithotrophic ferrous-oxidising bacterium *Thiobacillus ferrooxidans*. Journal of Bacteriology 182(12), 3602-3606.

Geankoplis, CJ., 1983. Transport Processes. Allyn-Bacon Inc.

Giudici-Orticoni, M-T., Guerlesquin, F., Bruschi, M., Nitschke, W., 1999. Interaction-induced redox switch in the electron transfer complex rusticyanin-cytochrome c4. Journal of Biological Chemistry 274(43), 30365-30369.

Ida, C., Sasaki, K.., Akikazu, A., Blake, R.C., Saiki, H., Ohmura, N., 2003. Kinetic rate constant for electron transfer between ferrous ions and novel Rusticyanin isoform in *Acidithiobacillus ferrooxidans*. Journal of Bioscience and Bioengineering 95, 534-537

Ingledew, J.W., Cobley, J.G., 1980. A potentiometric and kinetic study on the respiratory chain of ferrous-iron-grown *Thiobacillus ferrooxidans*. Biochimica et Biophysica Acta 590, 141-158.

Ingledew, W.J., Cox, J.C., Halling, P.J., 1977. A proposed mechanism for energy conservation during iron(II) oxidation by *Thiobacillus ferro-oxidans*: chemiosmotic coupling to net proton influx. FEMS Microbiology Letters 2(4), 193-7.

Jones, C.A., Kelly, D.P., 1983. Growth of *Thiobacillus ferrooxidans* on ferrous iron in chemostat culture: influence of product and substrate inhibition. Journal of Chemical. Technology and Biotechnology. 33B, 241-261.

Kazadi, T.K., Petersen, J., 2008. Kinetic measurement of biological oxidation of ferrous iron at low ferric to ferrous ratios in a controlled potential batch reactor. Hydrometallurgy 94(1-4), 48-53.

Kyritsis, P., Dennison, C., Ingledew, W.J., McFarlane, W., Sykes, A.G., 1995. Determination of the self-exchange rate constant for rusticyanin from *Thiobacillus ferrooxidans* a comparison with values for other type 1 blue copper proteins. Inorganic Chemistry 34(21), 5370-4.

Lide, D.R., (Ed.) 2005. CRC Handbook of Chemistry and Physics, Internet Version, <http://www.hbcpnetbase.com>, CRC Press, Boca Raton, FL.

Malarte, G., Leroy, G., Lojou, E., Abergel, C., Bruschi, M., Giudici-Orticoni, M-T., 2005. Insight into molecular stability and physiological properties of the diheme cytochrome CYC41 from the acidophilic bacterium *Acidithiobacillus ferrooxidans*. Biochemistry 44(17), 6471-6481.

May, N., Ralph, D.E., Hansford, G.S., 1997. Dynamic redox potential measurement for determining the ferric leach kinetics of pyrite. Minerals Engineering 10, 1279 –1290.

McGinnis, J., Ingledew, W.J., Sykes, A.G., 1986. Kinetic studies of 1:1 electron-transfer reactions of blue copper proteins. 13. Reactions of rusticyanin from *Thiobacillus ferrooxidans* with inorganic redox partners. Inorganic Chemistry 25(21), 3730-3733.

Millero, F.J., Huang, F., Graham, T.B., 2003. Solubility of oxygen in some 1-1, 2-1, 1-2 and 2-2 electrolytes as a function of concentration at 25°C. Journal of Solution Chemistry, 32(6), 473-487.

Meruane, G., Salhe, C., Wiertz, J., Vargas, T., 2002. Novel electrochemical-enzymatic model which quantifies the effect of the solution Eh on the kinetics of ferrous iron oxidation with *Acidithiobacillus ferrooxidans*. Biotechnology and Bioengineering 80(3), 280-288.

Nemati, M., Harrison, S.T.L., Hansford, G.S., Webb, C., 1998. Biological oxidation of ferrous sulfate by *Thiobacillus ferrooxidans*: a review on the kinetic aspects. Biochemical Engineering Journal 1(3), 171-190.

Ojumu, T.V., Petersen, J., Searby, G.E., Hansford, G.S., 2006. A review of rate equations proposed for microbial ferrous-iron oxidation with a view to application to heap bioleaching. Hydrometallurgy 83(1-4), 21-28.

Ojumu, T.V., Petersen, J., Hansford, G.S., 2008. The effect of dissolved cations on microbial ferrous-iron oxidation by *Leptospirillum ferriphilum* in continuous culture. Hydrometallurgy 94(1-4), 69-76.

Pirt, S.J., 1975. Principles of Microbe and Cell Cultivation. Blackwell Scientific, Oxford.

Robrish, S.A., LeRoy, A.F., Chassy, B.M., Wilson, J.J., Krichevsky, M.I., 1971. Use of a fibre optic probe for spectral measurements and the continuous recording of the turbidity of growing microbial cultures. Applied Microbiology 21, 278-287.

Rohwerder, T., Gehrke, T., Kinzler, K., Sand, W., 2003. Progress in bioleaching: fundamentals and mechanisms of bacterial metal sulfide oxidation. Bioleaching Review Part A:. Applied Microbiology and Biotechnology 63, 239–248

Shiers, D.W., Blight, K.R., Ralph, D.E., 2005. Sodium sulfate and sodium chloride effects on batch culture of iron-oxidizing bacteria. Hydrometallurgy 80(1-2), 75-82.

Sundkvist, J-E., Gahan, C.S., Sandstroem, A., 2007. Modeling of ferrous iron oxidation by a *Leptospirillum ferrooxidans*-dominated chemostat culture. Biotechnology Bioengineering 99(2), 378-389.

Trotman, RE. 1978. Technological Aids to Microbiology. Arnold, London.

von Stockar, U., Gustafsson, L., Larsson, C., Marison, I., Tissot, P., Gnaiger, E., 1993. Thermodynamic considerations in constructing energy balances for cellular growth. Biochimica et Biophysica Acta, Bioenergetics 1183(2), 221-40.

Table 1.

Redox electrode calibration constants in different media

Media	M00	M10	M20	M40
E^o (V)	0.664	0.661	0.637	0.625
RT/F (V)	0.0282	0.0262	0.0226	0.0250

Table 2.

Inoculation data from batch experiments in M00 medium.

	M00-17	M00-20	M00-22	M00-23	M00-24	M00-26
$N_0/10^8$ (cells L^{-1})	2.7	2.6	13	3.7	30	5.1
$E_{III/II}$ at inoculation (V)	0.570	0.561	0.574	0.566	0.592	0.591
time to oxidise 50% substrate (h)	24	27	18	26	17	20

Table 3.

Values for (dII/dt)/N from various sources.

Study	Given value	Given units	Converted value /10^{-13}	Comment
Kazadi et. Petersen (2008)	14	mmol(Fe) mmolC^{-1} h^{-1}	0.93	23.95 g(cells) mol C^{-1} and 1.0 g(cells) = 6.3×10^{12} cells*
Dempers et al. (2003)	12	mmol(Fe) mmolC^{-1} h^{-1}	0.80	
Ojumu et al. (2008)	20	mmol(Fe) mmolC^{-1} h^{-1}	1.33	
Breed et al. (1999)	8	mmol(Fe) mmolC^{-1} h^{-1}	0.53	
Sundkvist et al. (2007)	150	mg(Fe) μg protein^{-1} h^{-1}	0.002	assuming 1 g(protein) = 2 g(cells)
Meruane et al. (2002)	1.5×10^{-6}	μg(Fe) $cell^{-1}$ h^{-1}	0.27	
This study		**mol(Fe) $cell^{-1}$ h^{-1}**	**1.2**	

*From von Stockar et al. (1993), and Blight and Ralph (2008)

Figure 1. Substrate (II) and cell concentrations (N) in experiments 17 – 26 using M00 medium showing the effect of different inoculation numbers and initial $E_{III/II}$.

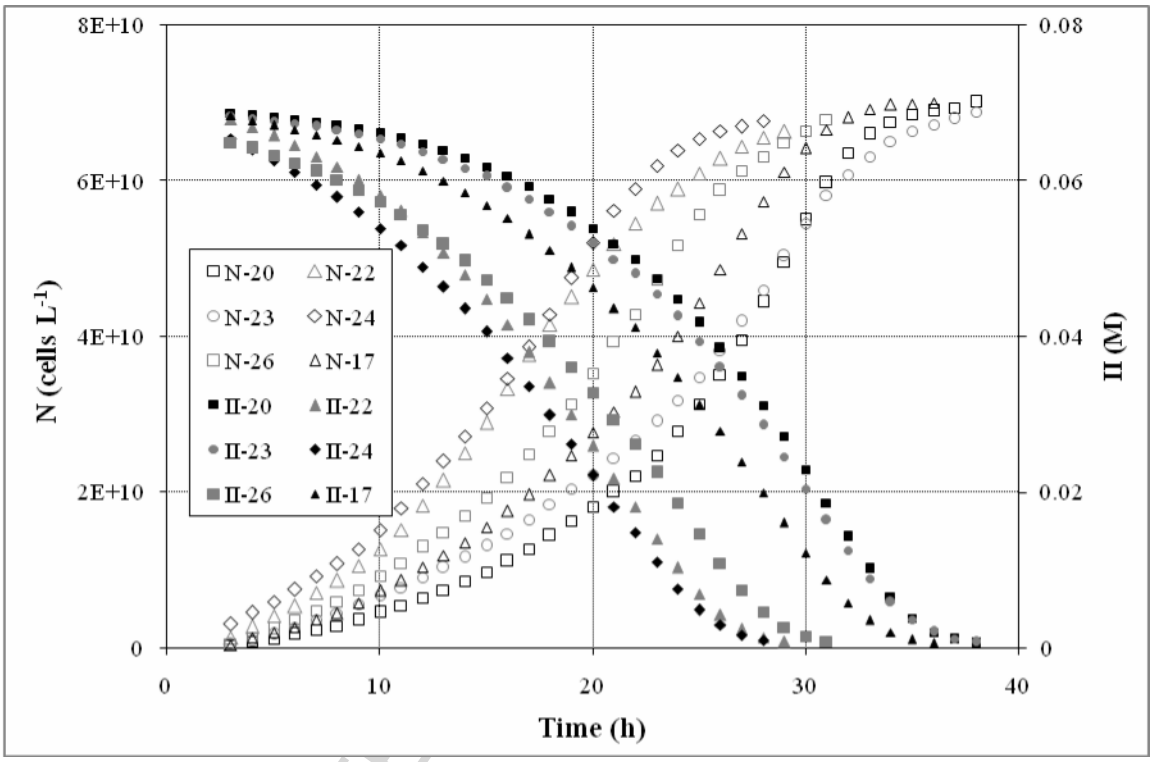

Figure 2. Specific iron oxidation rate as a function of [Fe^{2+}] experiments 17 - 26 using M00 medium showing the effect of different inoculation numbers and initial $E_{III/II}$.

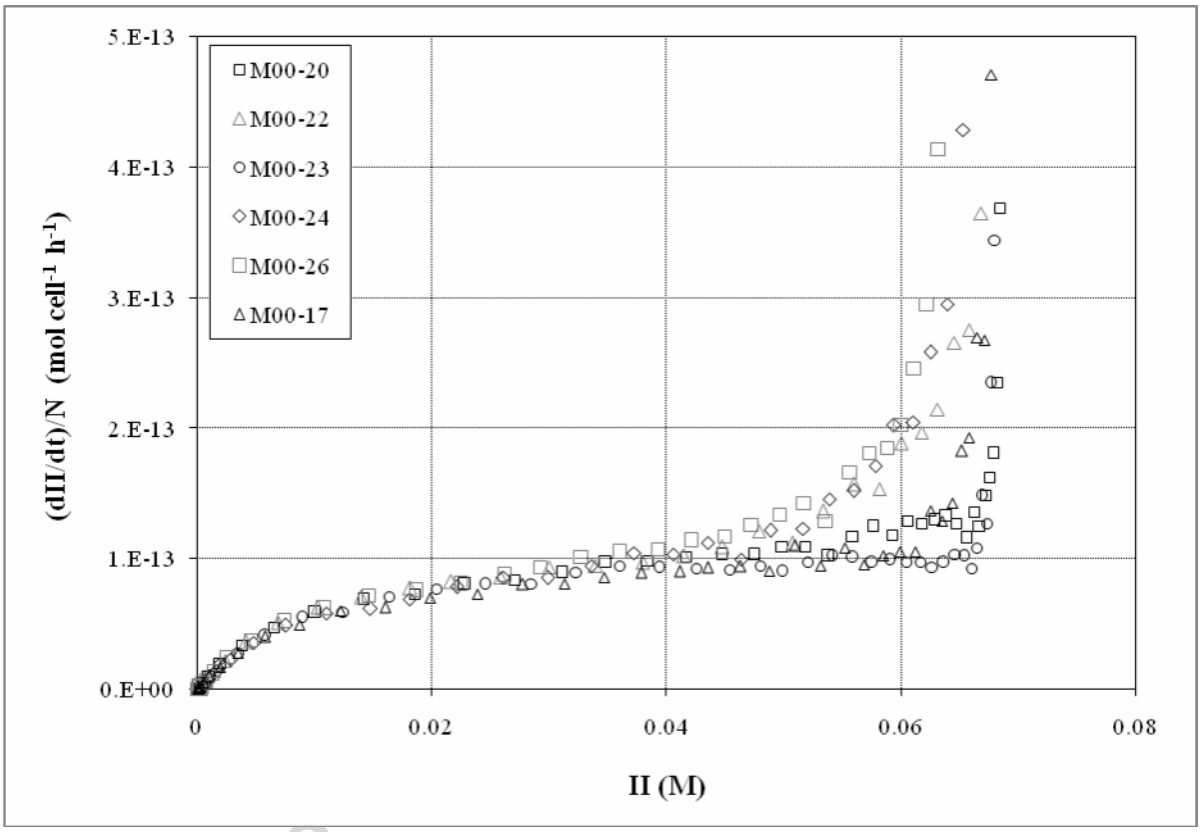

Figure 3. Specific iron oxidation rate as a function of $E_{III/II}$ in experiments 17 - 26 using M00 medium showing the effect of different inoculation numbers and initial $E_{III/II}$.

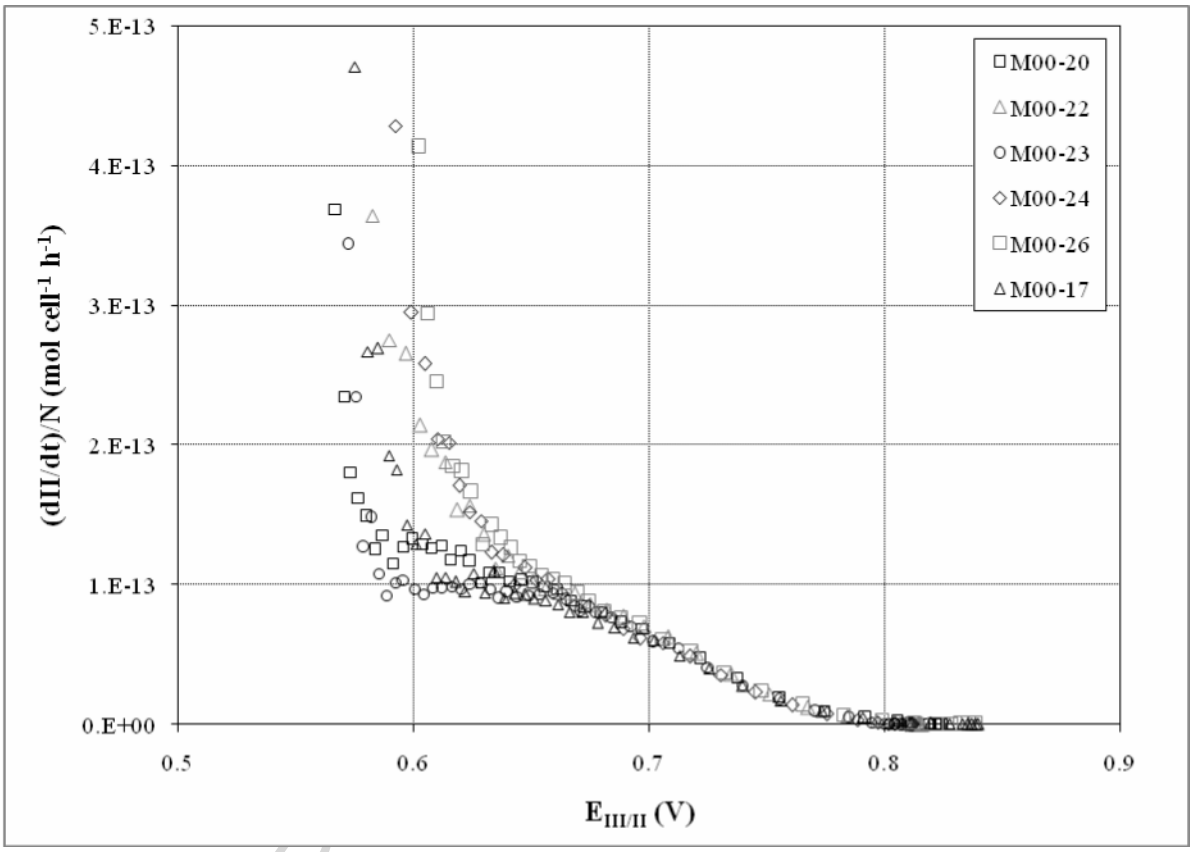

Figure 4. Specific cell growth rate as a function of $E_{III/II}$ in experiments 17 - 26 using M00 medium showing the effect of different inoculation numbers and initial $E_{III/II}$.

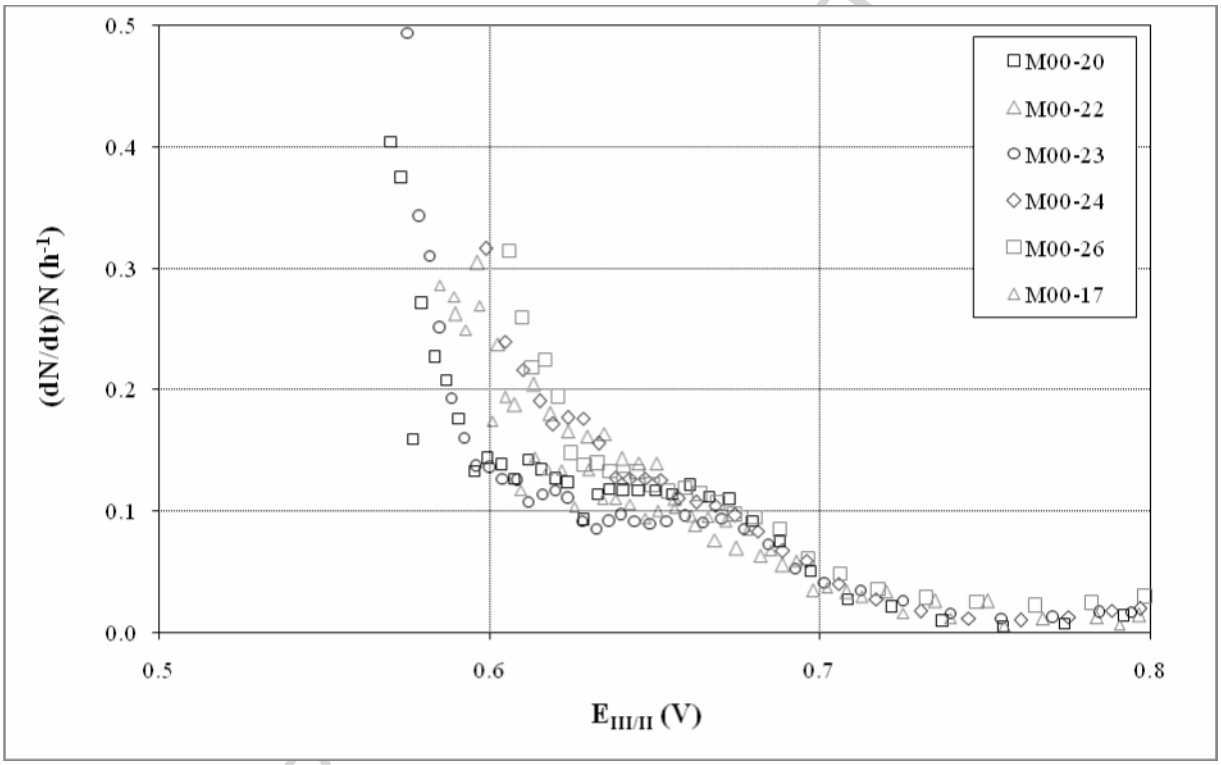

Figure 5. The Pirt equation applied to data from experiments 17 - 26 in M00 medium.

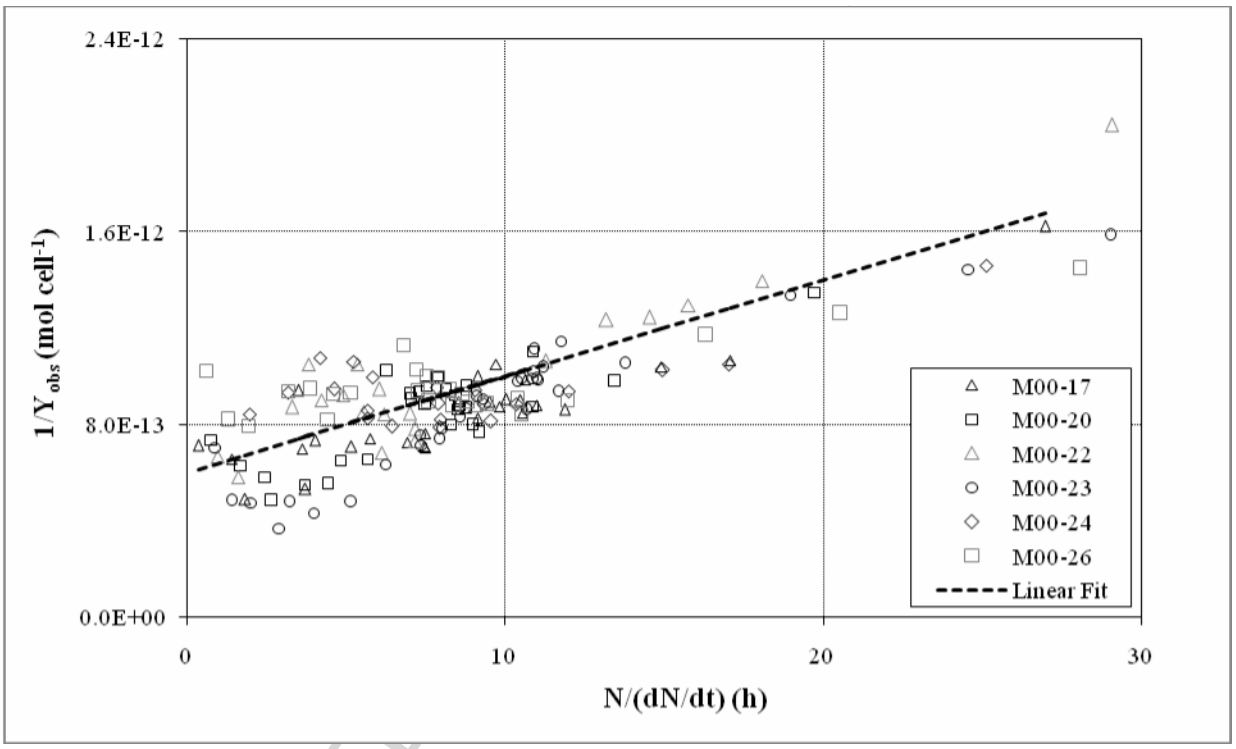

Figure 6. Instantaneous yields (Y_{obs}) in experiments 17 - 26 as a function of II in M00 medium.

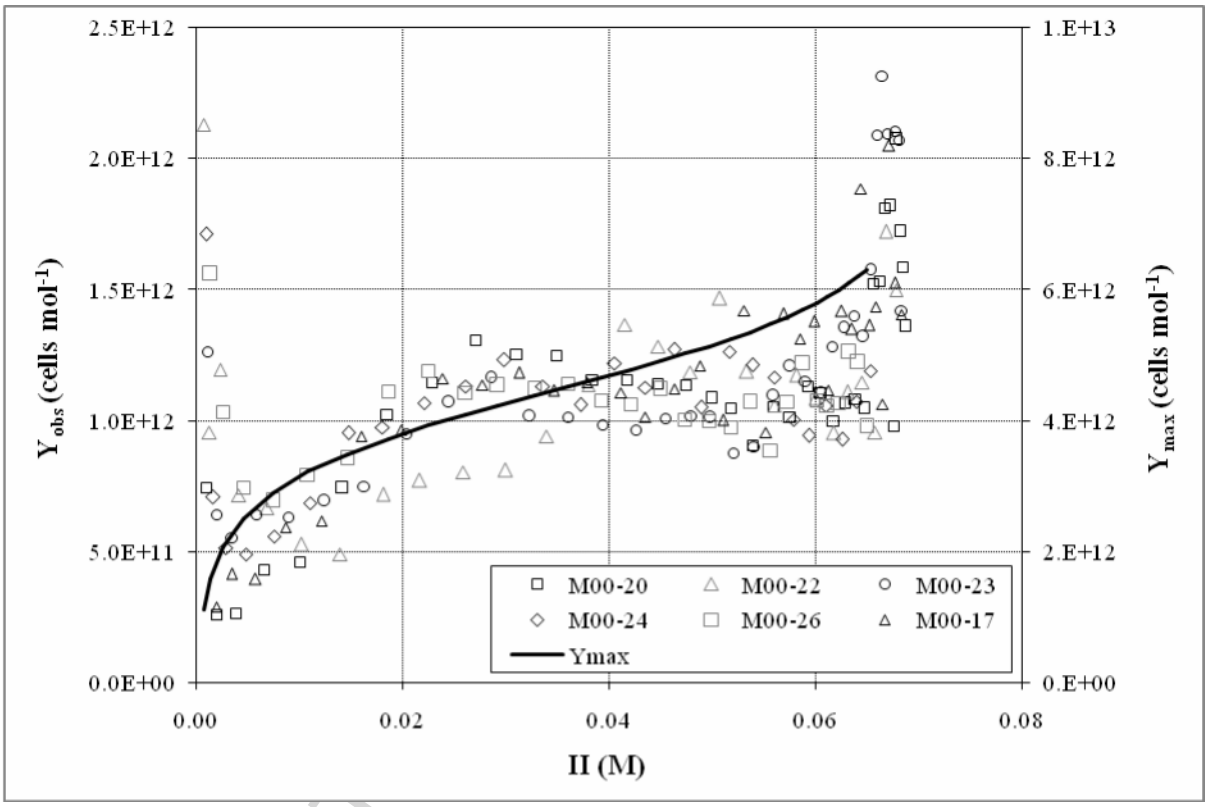

Figure 7. Instantaneous yields (Y_{obs}) in experiments 17 - 26 as a function of $E_{III/II}$ in M00 medium.

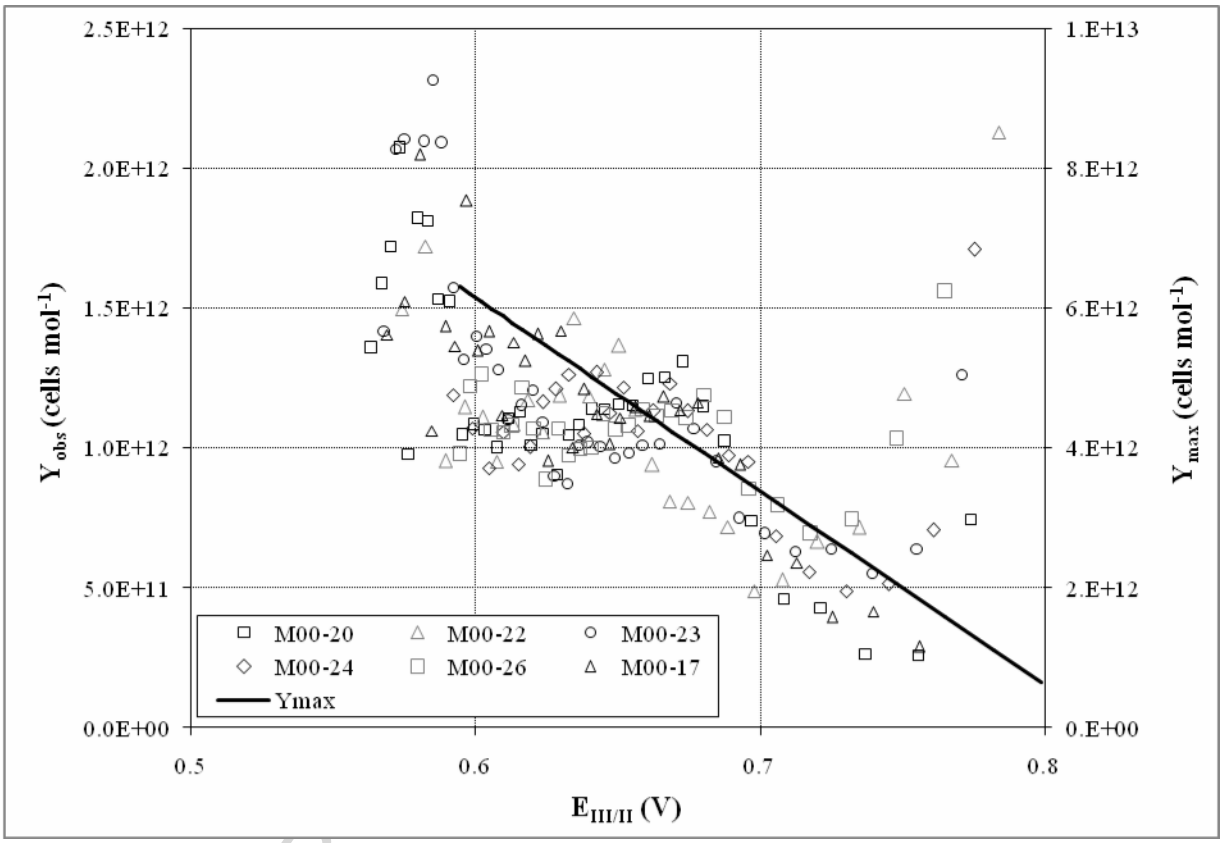

Figure 8. A comparison of batch culture experiments as the amount of sodium sulfate was increased (e.g. M40 included 40 g L^{-1}). Fe^{2+} (II) and cell concentrations (N) are shown.

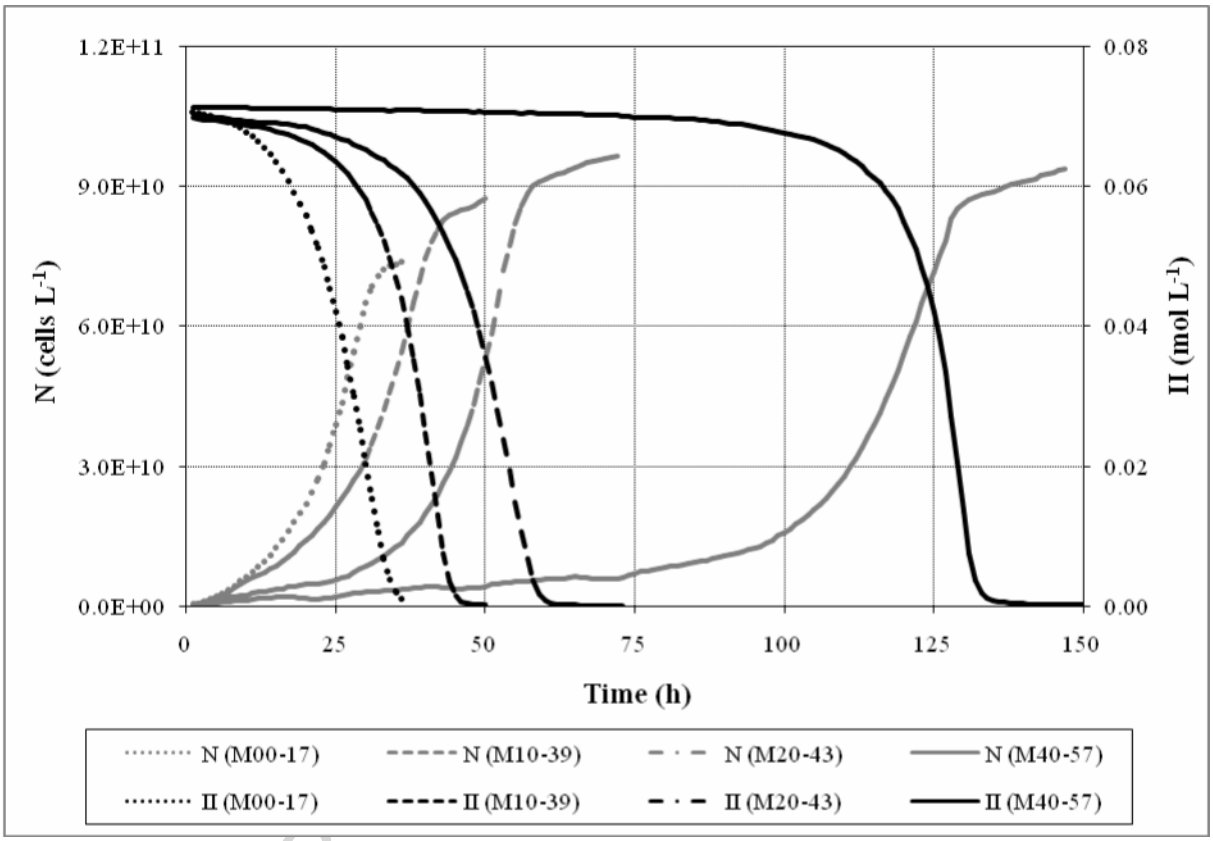

Figure 9. Substrate (II) and cell concentrations (N) in experiments 31, 39 and 41 using M10 medium showing the effect of different inoculation numbers and initial $E_{III/II}$.

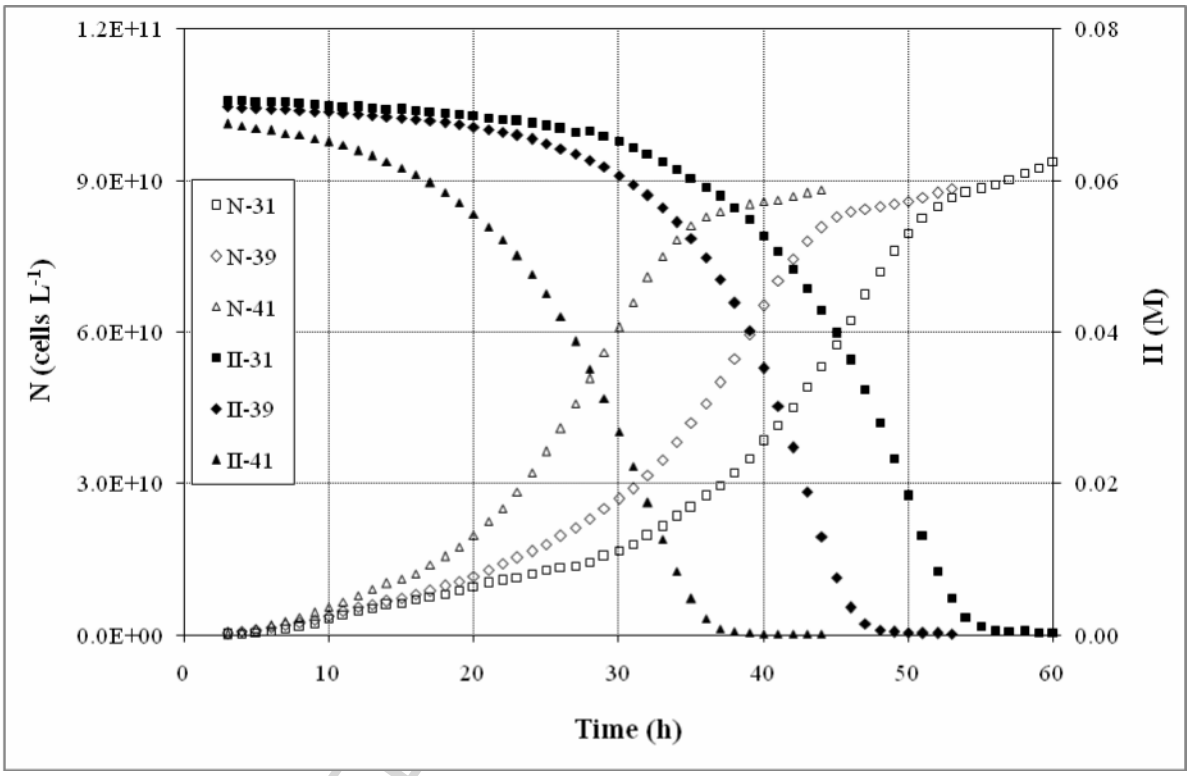

Figure 10. Specific iron oxidation rate as a function of $E_{III/II}$ in experiments 31, 39 and 41 using M10 medium showing the effect of different inoculation numbers and initial $E_{III/II}$.

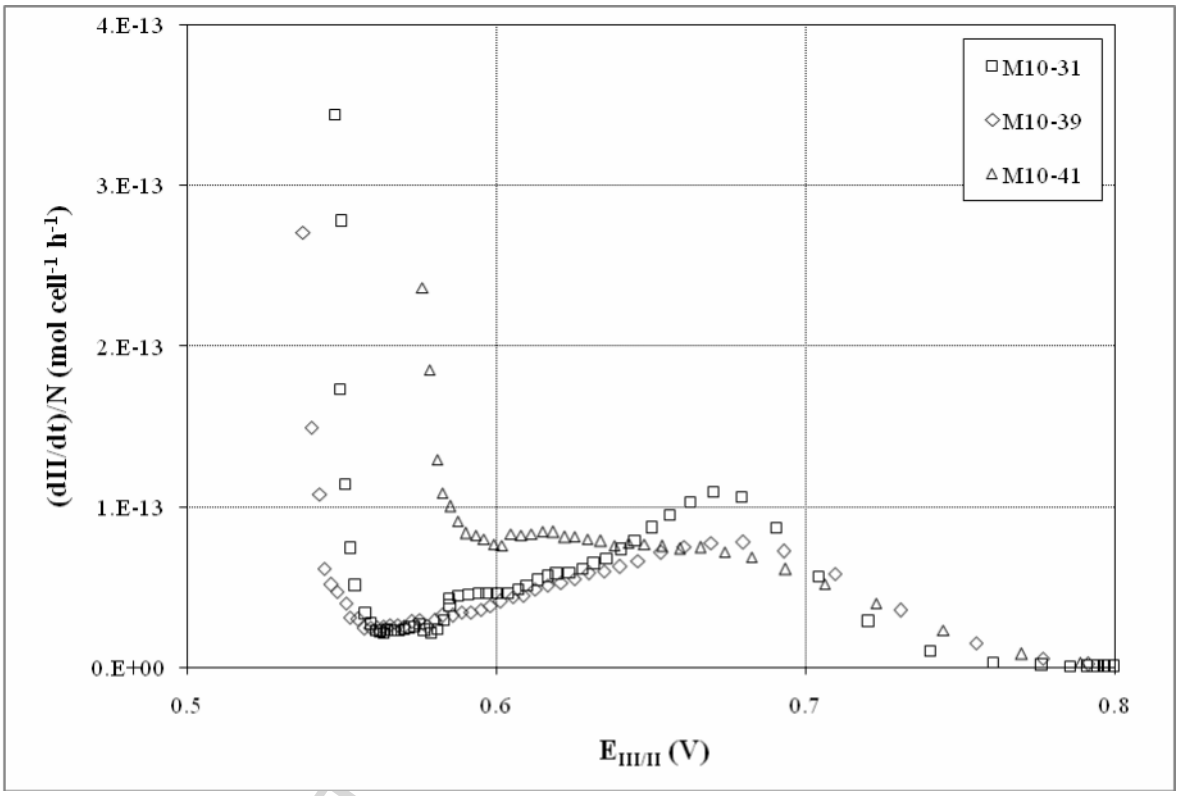

Figure 11. Iron oxidation rate as a function of $E_{III/II}$ in experiments using the four media. The initial $E_{III/II}$ value at inoculation is given in the legend.

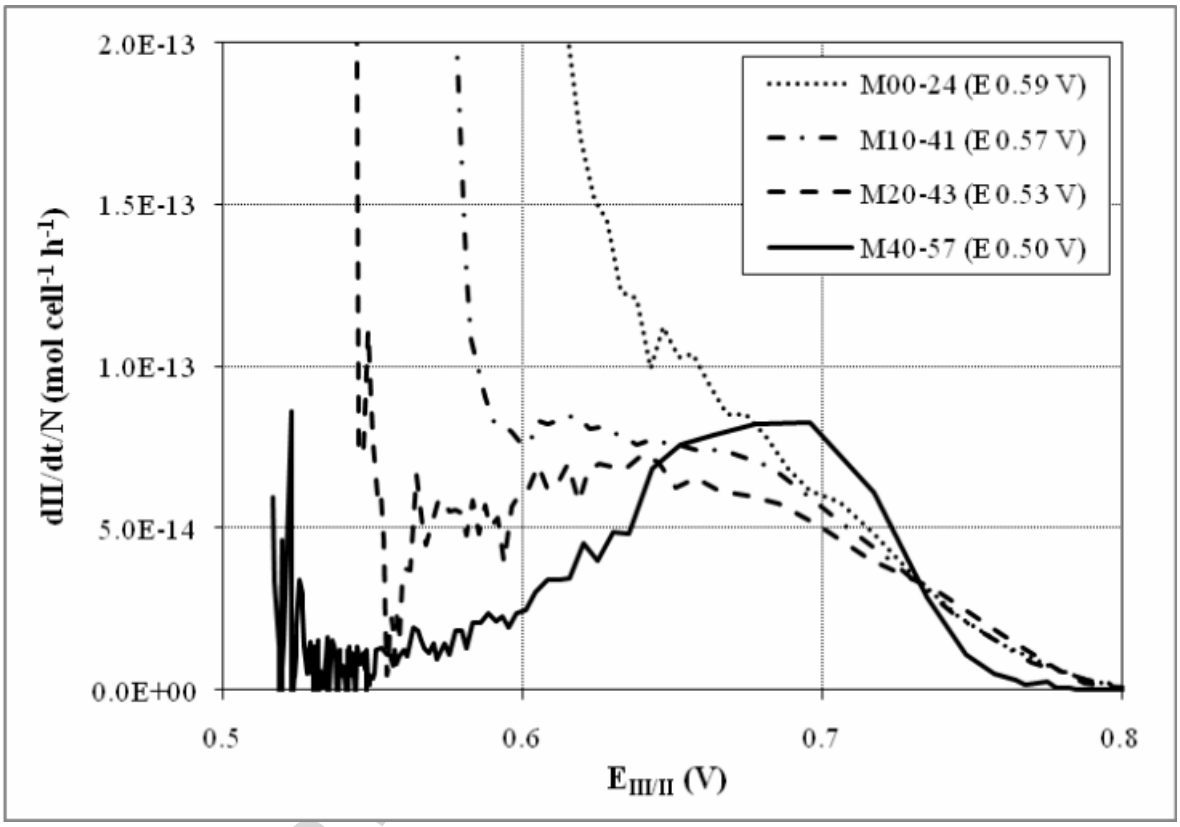

Figure 12. Specific substrate oxidation rates in the four media showing the effect of similar initial $E_{III/II}$ values.

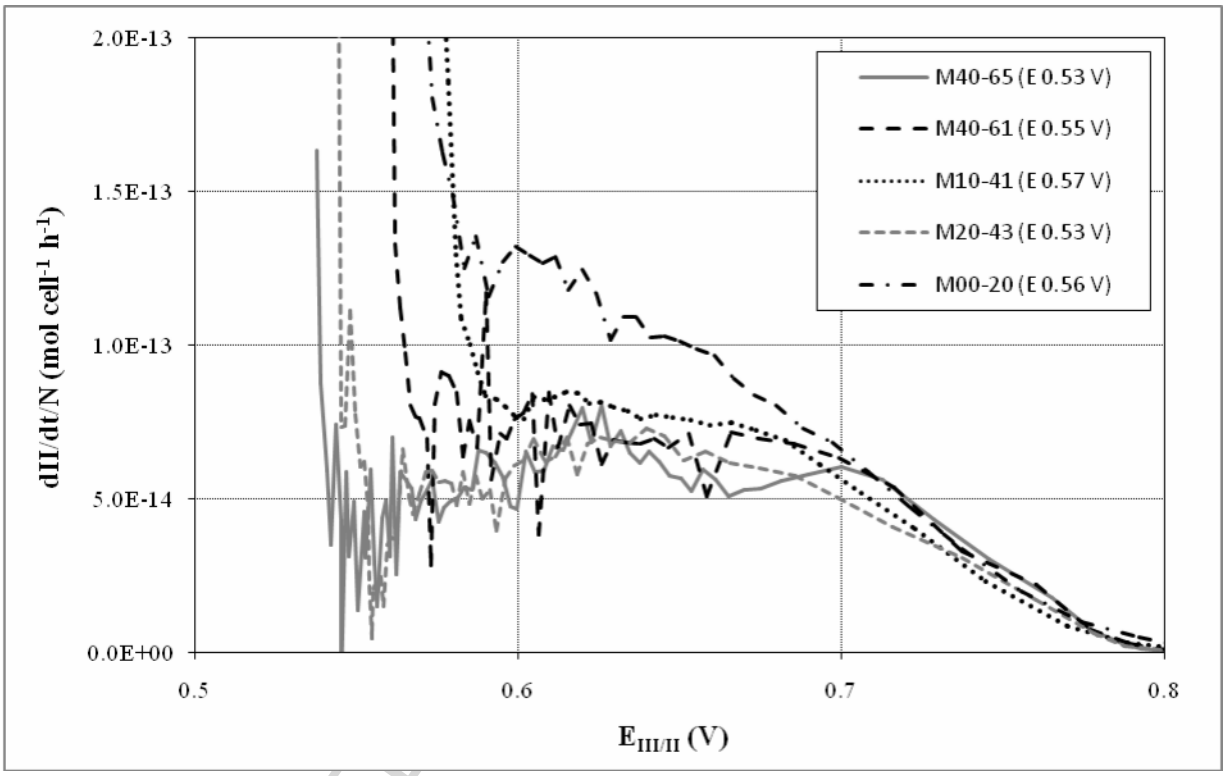

Figure 13. The single mediator rate limiting mechanism

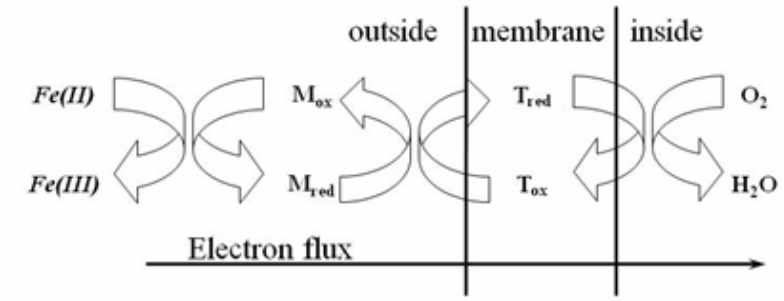

(Ingledew et al., 1977)

Figure 14. Idealised rate as a function of $E_{III/II}$ for a single 'rate limiting' mediator.